Supporting Information

Local Mutations can serve as a Game Changer for Global Protein Solvent Interaction

Ellen M. Adams[1], Simone Pezzotti[1], Jonas Ahlers[1], Maximilian Rüttermann[1], Maxim Levin[2], Adi Goldenzweig[3], Yoav Peleg[4], Sarel J. Fleishman[3], Irit Sagi[2], Martina Havenith[1]

[1]*Lehrstuhl für Physkalische Chemie II, Ruhr Universität Bochum, 44801 Bochum, Germany*

[2]*Department of Biological Regulation, Weizmann Institute of Science, Rehovot 7610001, Israel*

[3]*Department of Biomolecular Sciences, Weizmann Institute of Science, Rehovot 7610001, Israel*

[4]*Structural Proteomics Unit, Department of Life Sciences Core Facilities, Weizmann Institute of Science, Rehovot 7610001, Israel*

Table S1. MMP14 stability design PROSS parameters. [a] Numbering according to PDB entry 1BUV, chain M. [b] PROSS energy threshold of designs selected for experimental validation. [c] PROSS generated mutations, based on the human MMP14-WT, 1BUV, chain M sequence. [d] a PROSS suggested human to mouse mutation. [e]Residues that were mutated to match mouse MMP14-WT sequence identity, following manual inspection.The cutoffs defined the subsets of individually stabilizing mutations. Each defined subset resulted in a single variant. R.e.u, refers to Rosetta energy units. Figures in parentheses show the number of mutations.

Number of homologs in the alignment	441
Positions held fixed (R.e.u.)[a]	119,173,174,175,176,177,178,185,186,187,188,189,190,191,192,193,194,195,196,197,198,199,200,201,202,203,204,206,207,208,209,210,211,212,214,216,228,229,230,236,239,240,243,249,253,259,260,261,262,263
PROSS threshold[b]	-0.45 (14)

PROSS generated mutations[c] (reference: human MMP14-WT, 1BUV, 14 mutations)	I114L, L117K, Q120D, H121K, A139E, S153Q, E169D, H171R, S217A, E248G, S251N[d], A258Y, V270R, D273E
Manualy added mutations[e] (reference: human MMP14-WT, 1BUV, 3 mutations)	Y141F, G285S, E286K
MMP14-SA mutations (reference: human MMP14-WT, 17 mutations)	I114L, L117K, Q120D, H121K, A139E, Y141F, S153Q, E169D, H171R, S217A, E248G, S251N[d], A258Y, V270R, D273E, G285S, E286K
MMP14-SA mutations (reference: mouse MMP14-WT, 15 mutations)	I114L, L117K, Q120D, H121K, A139E, S153Q, E169D, H171R, L180F, S217A, Q224R, E248G, A258Y, V270R, D273E
MMP14-SIA mutations (reference: MMP14-SA)	H240E, E249H

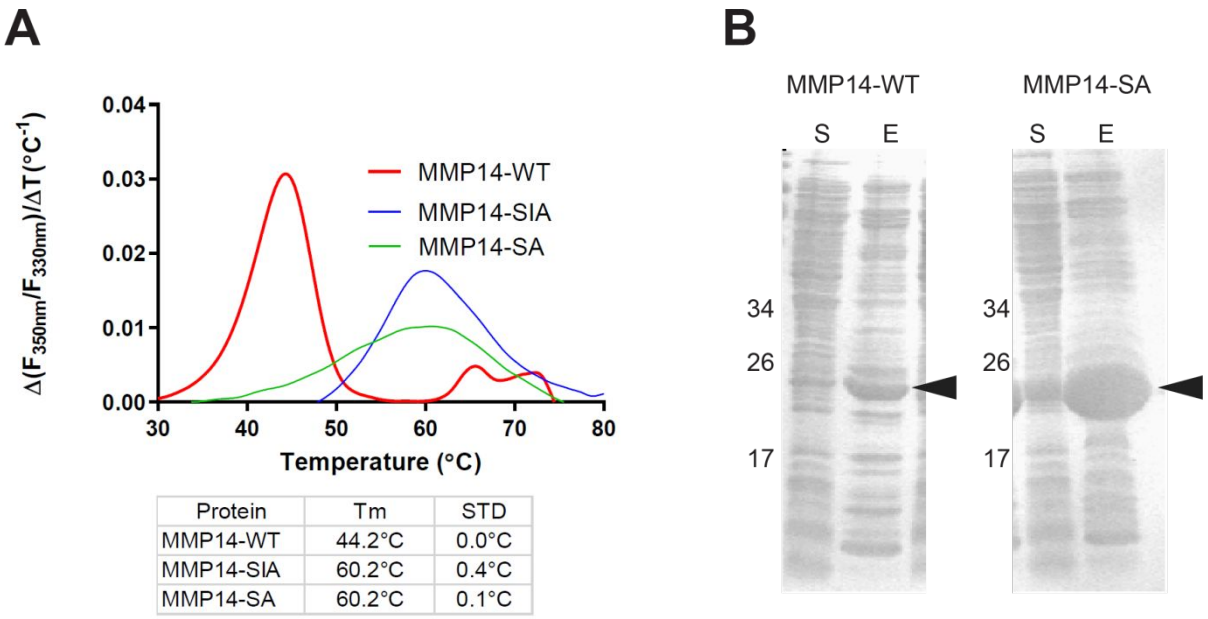

Figure S1. A: Differential scanning fluorimetry (DSF) stability analysis demonstrates enhanced stability of the mutants **B**: SDS-PAGE analysis of recombinant mouse MMP14-WT and MMP14-SA showing the expression of the proteins in the soluble fraction of cell lysates (S) and after elution in a NiNTA column (E). The SDS-PAGE is of the protein(s) prior to the purification process.

MMP14 Kinetic Assays

The assay was conducted on a fluorogenic peptide Mca-Pro-Leu-Gly-Leu-Dpa-Ala-Arg-NH_2, monitoring its hydrolysis at λ_{ex} = 340 nm and λ_{em} = 390 nm, as described previously,[1] with the following adaptations; assay conducted in 50 mM Tris-HCl buffer (pH 8 at 37 °C), 150 mM NaCl, 2.5 mM CaCl2, 2.5 μM ZnCl, and 0.01% Brij-35. Fluorescence was recorded immediately and continuously for 40 min at 37 °C. Initial reaction rates were measured, plotted, and analyzed using GraphPad Prism (version 8.0.0 for Windows, GraphPad Software, San Diego, California USA, www.graphpad.com)

The PROSS rationally designed mutations do not significantly impact the catalytic efficiency (k_{cat}/K_M) of the active mutant MMP14-SA relative to the wildtype MMP14-WT, as can be seen in Figure S2.

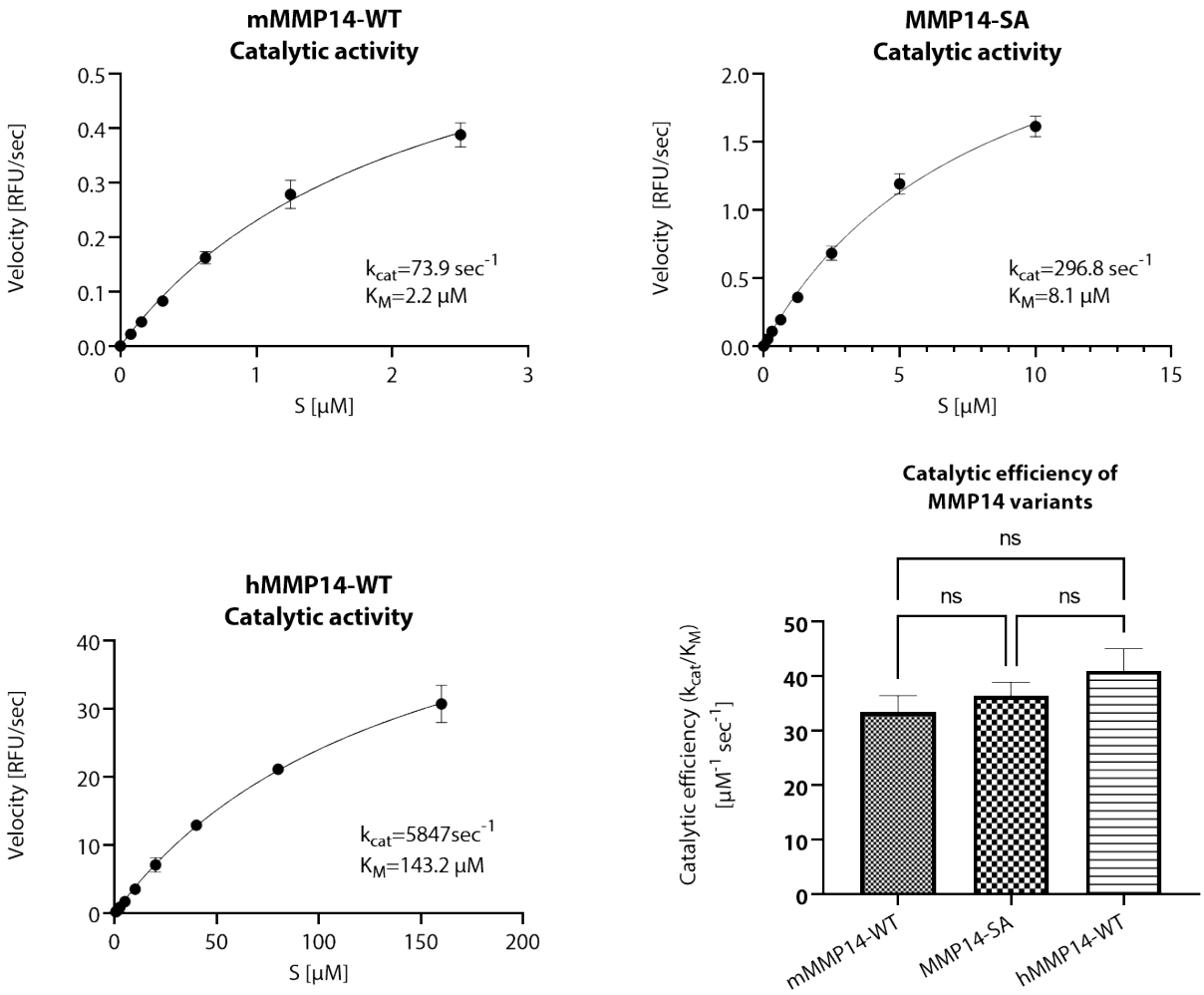

Figure S2. Michaelis–Menten kinetic analysis of hMMP14-WT, mMMP14-WT and MMP14-SA mutants on a standard MMP substrate. The calculated Michaelis constant (K_M) and the turnover number (k_{cat}) are specified in each analysis. In the lower panel, enzymes' catalytic efficiency was plotted and compared by an one way ANOVA test, showing no significant difference between the enzymes.

Simulation Details

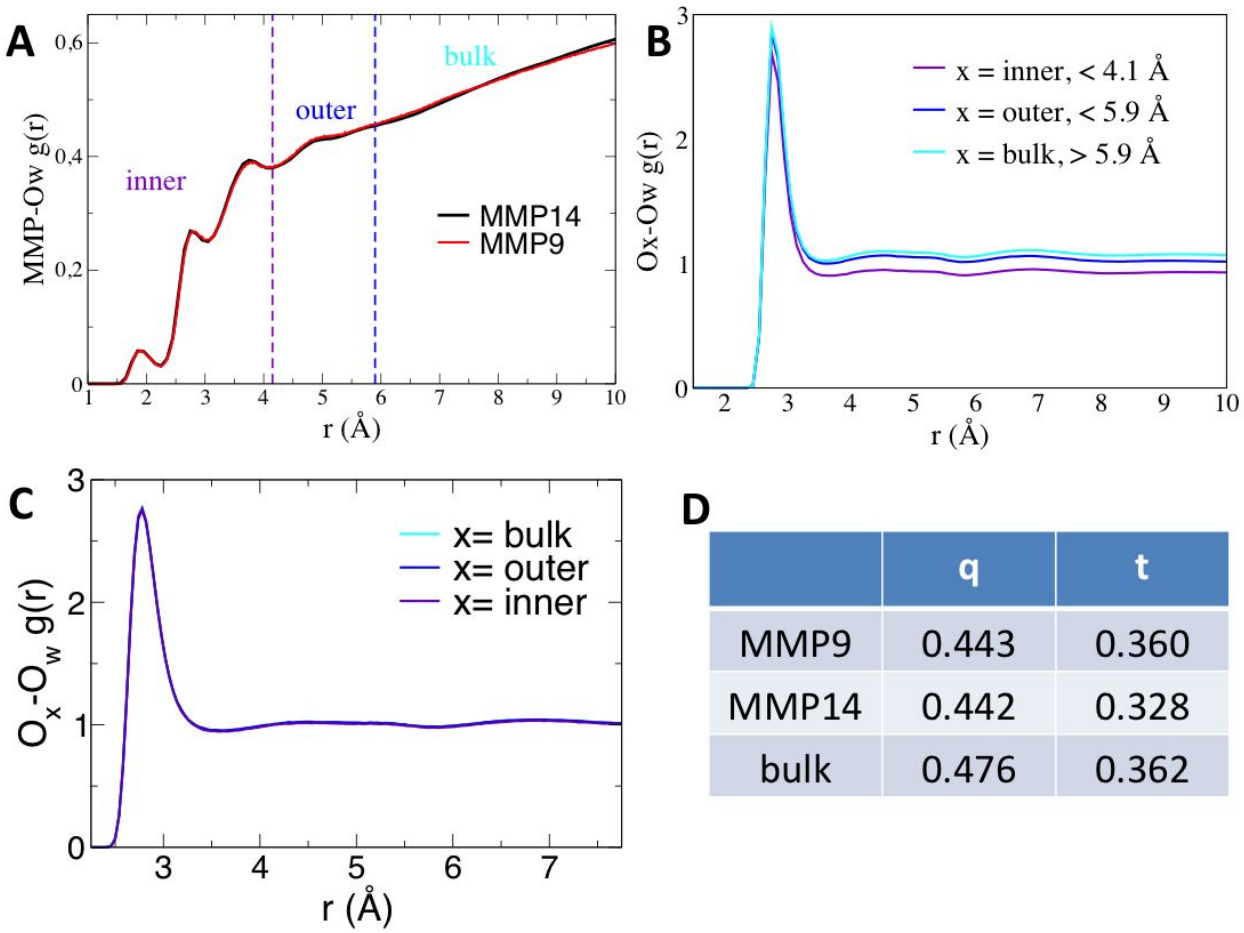

	q	t
MMP9	0.443	0.360
MMP14	0.442	0.328
bulk	0.476	0.362

Figure S3. A: radial pair distribution functions (g(r)) calculated in between all MMP14-WT (black) and MMP9-WT (red) atoms and all water molecules oxygen atoms (Ow). The vertical dashed lines identify the inner/outer/bulk regions as discussed in the text. **B:** oxygen-oxygen g(r) in between water molecules in each defined region and all water molecules in the simulation box for MMP14-WT (identical results are obtained for MMP14-SIA). C: same analysis performed on the MMP9-WT system. **D:** comparison between q and t order parameters for water in the inner layer around MMP14-WT and MMP9-WT.

Interestingly, both g(r) (Figure S3-B/C) and q/t order parameters (Figure S3-D) analysis reveal that MMP9-WT exhibits more bulk-like properties in the inner layer with respect to MMP14-WT and –SIA. This is in agreement with the experimental observations discussed in the main text.

Table S2 illustrates that the distinction into an inner hydration layer, structurally distinct from bulk water, and a "bulk-like" outer hydration layer, as discussed in the main text, holds true with respect to multiple descriptors.

Table S2. Average number of water-water HBs/molecule, q and t order parameters, and water dipole reorientation time (τ^{μ}, divided by the bulk reference, $\tau^{\mu}_{(bulk)}$), for water molecules in the inner hydration layer, outer hydration layer, and bulk regions (as defined in the main text and Figure S3). The reported values are for hydrated MMP14-WT. Similar values are obtained for MMP14-SIA (not shown). The total number of HBs/molecule formed in the inner layer increases to 2.97 when water-water HBs are added to water-MMP HBs (formed exclusively by bound water molecules).

Water region	Inner	Outer	Bulk
w-w HBs/molecule	**2.69**	**3.30**	**3.31**
q parameter	**0.442**	**0.474**	**0.476**
t parameter	**0.328**	**0.351**	**0.362**
$\tau^{\mu}/\ \tau^{\mu}_{(bulk)}$	**2.22**	**1.10**	**1.00**

q and t are two popular structural order parameters used to describe the structure, dynamics, and thermodynamics of bulk water over its phase diagram.[2]

The translational order parameter, t, is defined as

$$t = \frac{\int_0^{\xi_c} d\xi \, |g_{OO}(\xi) - 1|^2}{\xi_c} \qquad (1)$$

where g_OO (ξ) is the oxygen-oxygen radial distribution function, $\xi = r\rho^{(1/3)}$, r is the distance between the oxygen atoms of a pair of molecules, ρ is the bulk water density, and ξ_c is a cut-off distance, set to 3Å in this work. For an ideal gas, $g(\xi) = 1$ everywhere and t vanishes, whereas in a crystal there is long-range translational order, and $g(\xi) \neq 1$ over long distances and hence t is large.

The q parameter

$$q = 1 - \frac{3}{8} \sum_{i=1}^{3} \sum_{j=i+1}^{4} \left(cos\phi_{ij} - \frac{1}{3} \right)^2 \qquad (2)$$

measures tetrahedral order, where $\cos\phi_{ij}$ is the angle formed by the lines joining the oxygen atom of a given molecule and those of its nearest i,j neighbours (≤ 4). The average value of q varies between 0 (in an ideal gas) and 1 (in a perfect tetrahedral environment).

τ^{μ} values are obtained from the exponential fit of the orientational correlation function of the dipole vector of the water molecules in each defined inner/outer/bulk regions:

$$C_{\mu}^{(2)}(t) = \frac{\langle P_2[\mu(t) \cdot \mu(0)] \rangle}{\langle P_2[\mu(0) \cdot \mu(0)] \rangle} \qquad (3)$$

where P_2 is the 2nd rank Legendre polynomial and $\mu(t)$ is the water dipole moment (unit vector) at time t.[3]

TeraHertz Spectroscopy

Addition of a solute into the water solvent will result in a decrease in the THz absorption coefficient, due to replacement of a volume of water that is equal to the volume of the solute. This expected decrease of the solution absorption as a function of solute concentration, $\Delta\alpha(c)$, can be estimated by the relation $\Delta\alpha(c) = \alpha_{water} - (V_{solute}/V_{total})\alpha_{water}$, where V_{solute} is the volume of the solute in the total solution. In the case of proteins, V_{solute} can be determined from the protein radius of gyration (see Figure S3 for radius of gyration of MMP variants used here). While this is straight forward, any additional change upon addition of a solute can be due either to the low frequency absorption of the enzyme itself, e.g. intramolecular modes (which will increase the absorption) or by the hydration water, which might have an increased or decreased absorption compared to the bulk. The change compared to the bulk depends on the interactions with the protein, which may include changes in the surface electrostatic potential, or hydrophobic and hydrophilic interactions.

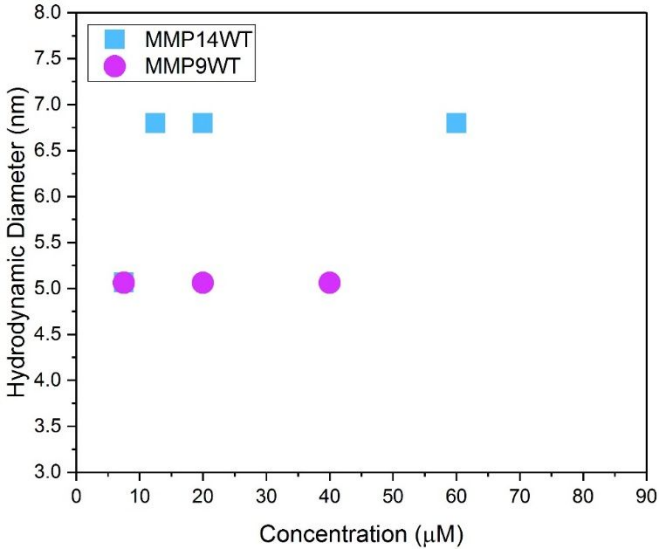

Figure S4. Hydrodynamic diameter of MMP14-WT and MMP9-WT in solution as a function of concentration measured by dynamic light scattering. The final hydrodynamic diameter was taken as the average value of all measurements and the radius of gyration was determined from the relation $R_g = 0.775R_H$.

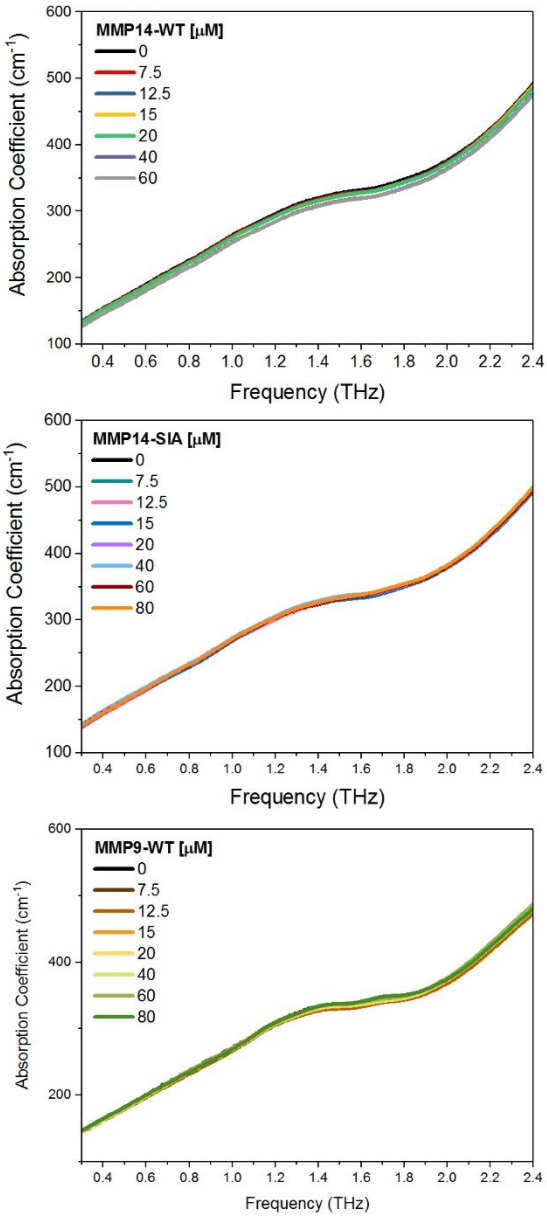

Figure S5. THz-TDS absorption spectra of MMP14-WT, MMP14-SIA, and MMP9-WT

REFERENCES SI

1 C. G. Knight, F. Willenbrock and G. Murphy, *FEBS Letters*, 1992, **296**, 263–266.
2 J. R. Errington and P. G. Debenedetti, *Nature*, 2001, **409**, 318–321.
3 S. Pezzotti, A. Serva and M.-P. Gaigeot, *The Journal of Chemical Physics*, 2018, **148**, 174701.